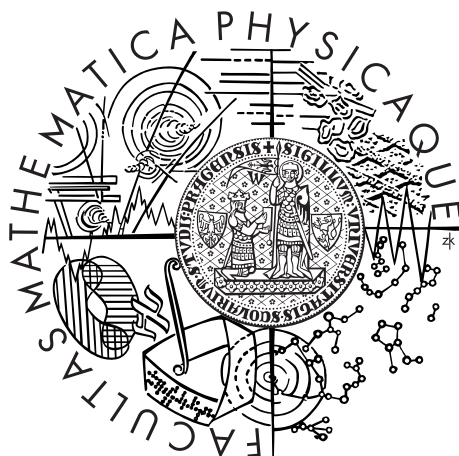


Univerzita Karlova v Praze  
Matematicko-fyzikální fakulta

## BAKALÁŘSKÁ PRÁCE



Tadeáš Dohnal

### Možnosti zkoumání oscilací elektronových (anti) neutrin z rozpadů mionů

Ústav částicové a jaderné fyziky

Vedoucí bakalářské práce: doc. RNDr. Rupert Leitner, DrSc.

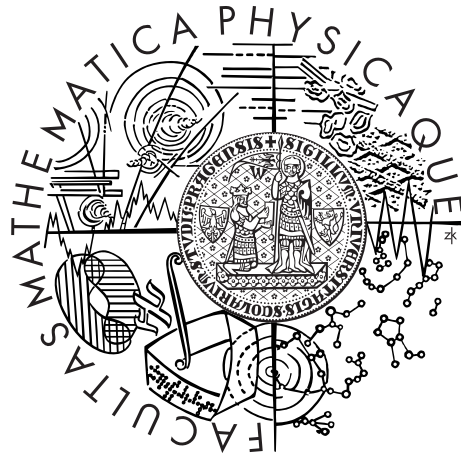
Studijní program: Fyzika

Studijní obor: Obecná fyzika

Praha 2014

Charles University in Prague  
Faculty of Mathematics and Physics

## BACHELOR THESIS



Tadeáš Dohnal

## Investigation of oscillations of electron (anti) neutrinos from muon decays

Institute of Particle and Nuclear Physics

Supervisor of the bachelor thesis: doc. RNDr. Rupert Leitner, DrSc.

Study programme: Physics

Specialization: General Physics

Prague 2014

I would like to thank my supervisor Rupert Leitner for introducing me to the interesting phenomenon of neutrino oscillations, my mother for helping me with English, Martin Mareš for creating the LaTeX template I used and many others for supporting me.

I declare that I carried out this bachelor thesis independently, and only with the cited sources, literature and other professional sources.

I understand that my work relates to the rights and obligations under the Act No. 121/2000 Coll., the Copyright Act, as amended, in particular the fact that the Charles University in Prague has the right to conclude a license agreement on the use of this work as a school work pursuant to Section 60 paragraph 1 of the Copyright Act.

In ..... date .....

signature of the author

Název práce: Možnosti zkoumání oscilací elektronových (anti) neutrin z rozpadů mionů

Autor: Tadeáš Dohnal

Katedra: Ústav částicové a jaderné fyziky

Vedoucí bakalářské práce: doc. RNDr. Rupert Leitner, DrSc., Ústav částicové a jaderné fyziky

Abstrakt: V této práci je zkoumán jev známý jako oscilace neutrin, a to v rámci modelu tří aktivních typů neutrin, který je popsán a s jehož pomocí jsou odvozeny pravděpodobnosti přechodu mezi jednotlivými typy neutrin. Dále je popsán efekt případného narušení CP-symetrie v oscilacích neutrin a jsou zváženy obtíže spojené s jeho měřením. Několik návrhů řešení těchto problémů je rozebráno, především pak koncept "továrny na neutrina" (tzn. využití neutrin z rozpadu mionů) tak, jak je to navrhováno v projektu nuSTORM. To zahrnuje i vlastní výpočet energetického spektra neutrin z rozpadu nepolarizovaného mionu (v klidu i v pohybu), úhlového rozdělení těchto neutrin a dalších specifikací.

Klíčová slova: neutrina, oscilace neutrin, miony

Title: Investigation of oscillations of electron (anti) neutrinos from muon decays

Author: Tadeáš Dohnal

Department: Institute of Particle and Nuclear Physics

Supervisor: doc. RNDr. Rupert Leitner, DrSc., Institute of Particle and Nuclear Physics

Abstract: In this thesis, the phenomenon of neutrino oscillations is investigated. General phenomenology for the three active neutrino framework is provided, along with transition probabilities in vacuum. The effect of eventual CP violation on neutrino oscillations and difficulties of its measurement are introduced. Several solutions are discussed, especially the concept of the neutrino factory (i.e. using neutrinos from muon decays) as it is projected by the nuSTORM collaboration. Energy spectra of neutrinos from unpolarized muon decays, both at rest and in flight are calculated, along with the angular distribution and other specifications.

Keywords: neutrinos, neutrino oscillations, muons

# Contents

<b>Introduction</b>	<b>2</b>
<b>1 Neutrino oscillations</b>	<b>4</b>
1.1 Brief historical background . . . . .	4
1.2 Mixing between flavour and mass eigenstates . . . . .	4
1.3 Propagation in vacuum and oscillations . . . . .	5
1.4 Oscillation parameters . . . . .	7
1.4.1 Measurement of $\theta_{12}$ and $\Delta m_{21}^2$ . . . . .	7
1.4.2 Measurement of $\theta_{23}$ and $\Delta m_{32}^2$ . . . . .	7
1.4.3 Measurement of $\theta_{13}$ . . . . .	8
1.4.4 Mass hierarchy and flavour content . . . . .	8
<b>2 CP and T violation in neutrino oscillations</b>	<b>10</b>
2.1 Effect on oscillation probabilities . . . . .	10
2.2 Measurement . . . . .	11
2.2.1 Threshold energies . . . . .	11
2.2.2 Neutrino-nucleon scattering cross section . . . . .	13
<b>3 Sterile neutrinos</b>	<b>15</b>
<b>4 Muons as a source of neutrinos</b>	<b>16</b>
4.1 Neutrino factory . . . . .	16
4.2 nuSTORM facility . . . . .	17
4.3 Decay of muon at rest . . . . .	18
4.4 Decay of muon in motion . . . . .	21
4.5 Decay of 3.8 GeV muon . . . . .	23
<b>Conclusion</b>	<b>26</b>
<b>Bibliography</b>	<b>27</b>

# Introduction

Neutrinos are elementary particles, to be more precise they are electrically neutral leptons. It was the famous problem of the continuous electron spectrum in beta decay, seemingly violating the conservation laws of energy and angular momentum, that led Wolfgang Pauli to postulate existence of a new particle, which he called *neutron* back then, in 1930 (the term *neutrino* was introduced few years later, when the neutron as we know it was discovered by J. Chadwick). Fortunately, his reluctance to conceive a particle that had not been observed before (and there was no certainty it would be ever observed) appeared to be vain. Nevertheless, it took many years until the first observation of neutrinos was made in mid-1950s [1]. Ever since, neutrinos have never ceased to surprise us.

As time passed, three generations of leptons have been discovered, each of them containing a charged lepton and a corresponding neutrino: the electron ( $e^-$ ) and the electron neutrino ( $\nu_e$ ) in the first generation, the muon ( $\mu^-$ ) and the muon neutrino ( $\nu_\mu$ ) in the second one, the tauon ( $\tau^-$ ) and the tauon neutrino ( $\nu_\tau$ ) in the third one. In addition to that, there is a corresponding antiparticle for each of those particles ( $e^+$ ,  $\bar{\nu}_e$ ,  $\mu^+$ ,  $\bar{\nu}_\mu$ ,  $\tau^+$ ,  $\bar{\nu}_\tau$ ).

While charged leptons interact via electromagnetic force, weak force and gravitation, neutrinos do not carry electric charge, so they interact only via weak force and gravitation. That makes them particularly difficult for observation. Moreover, there are hints that sterile neutrinos which do not even interact via weak force may exist.

Since we know that the lepton number of each generation is conserved in weak interactions, knowledge of flavours of charged leptons which take part in weak interactions provides us with knowledge of flavours of otherwise "invisible" neutrinos as well. For example in the pion decay  $\pi^+ \rightarrow \mu^+ + \nu$  the emitted neutrino must be  $\nu_\mu$  so that number of leptons in the second generation is conserved ( $0 = -1 + 1$ ) etc. However, it would not be neutrinos, if the situation regarding their flavours was that simple.

One of big questions of physics nowadays is the question of neutrino masses. At first it seemed (and Standard model said so) that neutrinos were massless (and they nearly are massless compared to other massive particles), but it revealed that they have tiny, yet nonzero masses which make the whole situation quite complicated. As neutrino oscillations proved, the neutrino flavour eigenstates are not even identical to the neutrino mass eigenstates. This fact causes that flavour of a neutrino can change as the neutrino propagates in space-time.

In the first part of this thesis, the formalism of neutrino oscillations will be introduced. We shall work in the three active neutrino framework using the PMNS mixing matrix in order to derive transition probabilities for neutrinos propagating in vacuum. Furthermore, current knowledge of oscillation parameters will be summarized, i.e. their values and brief explanations where they came from.

In the second part, we shall focus on CP violation (and associated T violation) in neutrino oscillations. We shall see how it may affect transition probabilities. We shall discuss the difficulties connected with the measurement of CP violation: threshold energies for production of a charged lepton and insufficient knowledge of a neutrino-nucleon scattering cross section, especially for electron (anti)neutrinos.

In the third part, possible existence of sterile neutrinos will be outlined by providing brief overview of experiments that can not be sufficiently explained in the three active neutrino framework.

And finally, we shall take a close look at the possibility of using muons as a source of neutrinos. The concept of *neutrino factory* will be described in general and one of the possible implementations, the nuSTORM facility, will be described in a bit more detail. Moreover, my own calculations of energy spectra of neutrinos emitted in muon decay will be presented, both for muons at rest and unpolarized muons in motion, especially for 3.8 GeV muons considered in the nuSTORM project. Along with that, angular specifications of neutrino beam will be described.

# 1. Neutrino oscillations

## 1.1 Brief historical background

The idea of neutrino oscillations (which requires neutrinos to have mass) was proposed in 1957 by Bruno Pontecorvo. About ten years later the solar neutrinos problem arose when only about one third of the theoretical flux was detected. The idea of oscillations was reviewed as an explanation of the deficit. The first compelling evidence for neutrino oscillations was provided in 1998 by the Super-Kamiokande experiment measuring atmospheric neutrinos. Since then, many experiments investigating neutrino oscillations have been carried out and they have brought more light to this interesting phenomenon. However, many questions still remain unanswered (more about history can be found in [1, 2]).

## 1.2 Mixing between flavour and mass eigenstates

The basic idea behind neutrino oscillations is that the neutrino flavour eigenstates  $|\nu_\alpha\rangle$  are not identical to the neutrino mass eigenstates  $|\nu_i\rangle$ . In case of no sterile neutrinos (possibility of existence of sterile neutrinos will be discussed later) there are three flavour eigenstates: the electron, muon and tauon neutrino which are produced (or absorbed) in weak interactions. If neutrinos are Dirac particles, the lepton number of each generation in these interactions is conserved (an electron neutrino is produced with a positron or absorbed to produce an electron and so on). For Majorana neutrinos (in such case the neutrino would be its own antiparticle), this rule may be violated. Either way, we can write:

$$|\nu_\alpha\rangle = \sum_{i=1}^3 U_{\alpha i}^* |\nu_i\rangle \quad (1.1)$$

where  $U$  is the so-called Pontecorvo-Maki-Nakagawa-Sakata (PMNS) matrix (description of this formalism can be found in [1, 2, 3, 4, 5]). Its elements can be written in a way:

$$U_{\alpha i} \equiv \langle \nu_\alpha | \nu_i \rangle \quad (1.2)$$

By using the CPT symmetry we get analogous expression for antineutrinos as well:

$$\bar{U}_{\alpha i} \equiv \langle \bar{\nu}_\alpha | \bar{\nu}_i \rangle = \langle \nu_i | \nu_\alpha \rangle \equiv U_{\alpha i}^* \quad (1.3)$$

If there were generally  $n$  neutrino species, PMNS matrix would be a  $n \times n$  complex unitary matrix. Such a matrix is determined by  $n^2$  independent parameters. However,  $n$  phases of charged leptons can be redefined in order to remove  $n$  parameters. If neutrinos are Dirac particles, additional  $(n - 1)$  relative phases of  $n$  neutrino states can be redefined as well to remove  $(n - 1)$  more parameters. That leaves the PMNS matrix with  $(n - 1)^2$  parameters. In case of Majorana neutrinos the later redefinition is not possible and the PMNS matrix has  $n(n - 1)$  parameters, but the additional Majorana phases do not affect neutrino oscillations. Either way, it follows that neutrino oscillations depend on  $(n - 1)^2$  parameters [4].

In case of three known active neutrino species (which is the framework we will use), there are 4 parameters in the PMNS matrix which interest us. The usual way is to write the PMNS matrix in terms of three mixing angles  $\theta_{12}$ ,  $\theta_{13}$ ,  $\theta_{23}$  and one possibly CP and T symmetry violating phase  $\delta$ :

$$U_{\alpha i} = \begin{pmatrix} 1 & 0 & 0 \\ 0 & c_{23} & s_{23} \\ 0 & -s_{23} & c_{23} \end{pmatrix} \begin{pmatrix} c_{13} & 0 & s_{13}e^{i\delta} \\ 0 & 1 & 0 \\ -s_{13}e^{-i\delta} & 0 & c_{13} \end{pmatrix} \begin{pmatrix} c_{12} & s_{12} & 0 \\ -s_{12} & c_{12} & 0 \\ 0 & 0 & 1 \end{pmatrix} D_M(\alpha_1, \alpha_2) \quad (1.4)$$

where  $s_{ij}$  stands for  $\sin(\theta_{ij})$  and  $c_{ij}$  for  $\cos(\theta_{ij})$ ;  $D_M$  denotes diagonal matrix including two Majorana phases  $\alpha_1$ ,  $\alpha_2$  in case of the Majorana origin of neutrinos (whether neutrinos are Dirac or Majorana particles it remains unclear). Since these phases do not affect neutrino oscillations, we will not use them in further calculations.

### 1.3 Propagation in vacuum and oscillations

In this section we will look at propagation of neutrinos in vacuum [1, 2, 3, 4, 5].

Assuming that all neutrinos we actually deal with are highly relativistic (because of their tiny mass), we can establish a simple relation between the distance travelled  $L$  and time  $t$ :  $L = tc$ . Another advantage of this approach is the simplification of the formula for energy of a neutrino:

$$E_i = \sqrt{p_i^2 + m_i^2} \cong p_i + \frac{m_i^2}{2E_i} \quad (1.5)$$

where  $E_i$ ,  $p_i$  and  $m_i$  denote the energy, momentum and mass of  $|\nu_i\rangle$  respectively. The other assumption we shall make is that the propagating neutrino can be described as a plane wave for which we can state:

$$|\nu_i(t, L)\rangle = e^{-\frac{i}{\hbar}E_it} e^{+\frac{i}{\hbar}p_iL} |\nu_i\rangle \quad (1.6)$$

That leads to the formula for evolution of a flavour eigenstate:

$$|\nu_\alpha(t, L)\rangle = \sum_{i=1}^3 U_{\alpha i}^* |\nu_i(t, L)\rangle \quad (1.7)$$

Now we can derive the probability  $P_{\alpha\beta}$  of finding (measuring) a neutrino in the flavour eigenstate  $|\nu_\beta\rangle$  whereas the eigenstate in which the neutrino was created is  $|\nu_\alpha\rangle$ .  $P_{\alpha\beta}$  denotes analogous probability for antineutrinos. Those probabilities are subject of neutrino oscillation experiments.

$$P_{\alpha\beta} = |\langle \nu_\beta | \nu_\alpha(t, L) \rangle|^2 = \left| \sum_{i=1}^3 \sum_{j=1}^3 U_{\alpha i}^* U_{\beta j} \langle \nu_j | \nu_i(t, L) \rangle \right|^2 \quad (1.8)$$

This is valid even without simplifications made above, however those simplifications are very useful to evaluate the probability  $P_{\alpha\beta}$  using  $L$ ,  $E$  and  $m_i$  or, to be more precise, the difference between square of masses of neutrino mass eigenstates:

$$\Delta m_{ij}^2 \equiv m_i^2 - m_j^2 \quad (1.9)$$

Taking into account the simplifications made above, we can rewrite the expression (1.8) to the form:

$$P_{\alpha\beta} = \sum_{i=1}^3 \sum_{j=1}^3 e^{-i\phi_{ij}(L,t)} U_{\alpha i}^* U_{\beta i} U_{\alpha j} U_{\beta j}^* \quad (1.10)$$

where  $\phi_{ij}(t, L)$  is a relative phase factor caused by different propagation of particular neutrino mass eigenstates  $|\nu_i\rangle$ :

$$\phi_{ij}(t, L) = \frac{(E_i - E_j)ct - (p_i - p_j)L}{\hbar c} \cong \frac{(m_i^2 - m_j^2)L}{2E\hbar c} \equiv \frac{\Delta m_{ij}^2 L}{2E\hbar c} \quad (1.11)$$

Further alterations can be applied to the formula (1.10) in order to obtain the final expression:

$$P_{\alpha\beta} = \delta_{\beta\alpha} - 4 \sum_{i<j} \text{Re}[U_{\alpha i}^* U_{\beta i} U_{\alpha j} U_{\beta j}^*] \sin^2 \left( \frac{\Delta m_{ij}^2 L}{4E\hbar c} \right) + \\ + 2 \sum_{i<j} \text{Im}[U_{\alpha i}^* U_{\beta i} U_{\alpha j} U_{\beta j}^*] \sin \left( \frac{\Delta m_{ij}^2 L}{2E\hbar c} \right) \quad (1.12)$$

The first two terms of Eq. (1.12) are affected neither by interchange of the initial and final neutrino state ( $P_{\alpha\beta} = P_{\beta\alpha}$ , T-symmetry) nor by interchange of neutrino and antineutrino ( $P_{\alpha\beta} = P_{\alpha\beta}^*$ , CP-symmetry).

The third term of Eq. (1.12) is nonzero only if the CP- and T-symmetry is violated in neutrino oscillations which means that the PMNS matrix is complex due to the  $\delta \neq 0$ . In that case  $P_{\alpha\beta} \neq P_{\beta\alpha}$ ,  $P_{\alpha\beta} \neq P_{\alpha\beta}^*$ ; however CPT-symmetry grants  $P_{\alpha\beta} = P_{\beta\alpha}^*$ .

Let us focus on the CP conserving part (the first two terms of Eq. (1.12)), the CP violating part will be discussed later. As we can see the transition probability  $P_{\alpha\beta}$  has an oscillatory behaviour with the distance between two maxima (or minima) measured in  $L/E$  dependant on the difference of squares of neutrino masses  $\Delta m_{ij}^2$ :

$$\frac{L}{E} = \frac{4\pi\hbar c}{\Delta m_{ij}^2} \quad (1.13)$$

We can also evaluate constants in the phase factor  $\phi_{ij}$  to get:

$$\frac{\phi_{ij}}{2} \equiv \frac{\Delta m_{ij}^2 L}{4E\hbar c} \doteq 1.27 \left( \frac{\Delta m_{ij}^2}{\text{eV}^2} \right) \left( \frac{L}{\text{km}} \right) \left( \frac{\text{GeV}}{E} \right) \quad (1.14)$$

In experiments, a common choice is to place a detector to the first disappearance minimum (appearance maximum) for which the following formula applies (using the same units as in (1.14)):

$$\frac{L}{E} = \frac{\pi}{2.54\Delta m_{ij}^2} \quad (1.15)$$

## 1.4 Oscillation parameters

This section is based on the information from [1, 3, 6, 7].

Neutrino oscillations and parameters that determine them are a subject to continuous and intense research. The reason is that many questions still remain unanswered and our current state of knowledge is incomplete and may be overcome in the near future.

As we can see in Eq. (1.12), the parameters playing a role in neutrino oscillations are three mixing angles ( $\theta_{12}$ ,  $\theta_{13}$ ,  $\theta_{23}$ ), one CP-violating phase ( $\delta$ ) and three mass differences ( $\Delta m_{21}^2$ ,  $\Delta m_{31}^2$ ,  $\Delta m_{32}^2$ ), although only two of those differences are independent:  $\Delta m_{31}^2 = \Delta m_{32}^2 + \Delta m_{21}^2$ .

The current knowledge of the mass splitting and mixing angles stems from experiments measuring solar neutrinos ( $\nu_e$  originating in solar thermonuclear reactions), reactor neutrinos ( $\bar{\nu}_e$  produced in beta decays in nuclear reactors, atmospheric neutrinos produced in atmosphere when cosmic rays hit it ( $\nu_\mu$ ,  $\bar{\nu}_\mu$ ,  $\nu_e$ ,  $\bar{\nu}_e$  as subsequent decay products of pions, muons, kaons etc.) and accelerator neutrinos (currently  $\nu_\mu$ ,  $\bar{\nu}_\mu$  from pion decays).

### 1.4.1 Measurement of $\theta_{12}$ and $\Delta m_{21}^2$

The Sun produces a calculable flux of  $\nu_e$ , but only a fraction of it is measured; this famous solar neutrino deficit led to the introduction of neutrino oscillations. Due to smallness of the  $\theta_{13}$  angle, oscillations of solar neutrinos are mostly determined by  $\theta_{12}$  and  $\Delta m_{21}^2$ . That allows us to calculate the survival probability in the two neutrino approximation [1]:

$$P_{ee}(L/E) = 1 - \sin^2(2\theta_{sol}) \sin^2\left(\frac{\Delta m_{sol}^2 L}{4E\hbar c}\right) \quad (1.16)$$

where  $\Delta m_{sol}^2 \cong \Delta m_{21}^2$  and  $\theta_{sol} \cong \theta_{21}$ . It has revealed that  $\Delta m_{21}^2 \approx 7.5 \cdot 10^{-5} \text{eV}^2$  (for precise values of oscillation parameters see Tab. 1.1) which places the first disappearance minimum of  $\nu_e$  and  $\bar{\nu}_e$  to the distance of 16.4 km/MeV. Besides, it has been found out that the mixing angle  $\theta_{12} \approx 34^\circ$ .

Together with experiments with solar  $\nu_e$  (Homestake, GALLEX, SAGE, SNO), experiments with reactor  $\bar{\nu}_e$  (KamLAND) provided valuable measurements leading to determination of those parameters.

### 1.4.2 Measurement of $\theta_{23}$ and $\Delta m_{32}^2$

The gap that separates  $m_3^2$  from  $m_2^2$  and  $m_1^2$  is about  $30\times$  bigger than the one that separates  $m_2^2$  and  $m_1^2$  so that it is often stated:

$$7.5 \cdot 10^{-5} \text{eV}^2 \approx \Delta m_{sol}^2 = \Delta m_{21}^2 \ll |\Delta m_{31}^2| \cong |\Delta m_{32}^2| \cong |\Delta m_{atm}^2| \approx 2.4 \cdot 10^{-3} \text{eV}^2 \quad (1.17)$$

$\Delta m_{sol}^2$  places the first disappearance minimum to the distance of 0.5 km/MeV. It was the Super-Kamiokande (SK-I) experiment measuring atmospheric neutrinos that provided the first compelling evidence for neutrino oscillations in 1998. Atmospheric neutrinos are  $\nu_\mu$ ,  $\bar{\nu}_\mu$ ,  $\nu_e$ ,  $\bar{\nu}_e$  produced in decays of pions, kaons (and subsequent muons) which are produced in upper atmosphere by interactions of primary cosmic rays. Although the  $\nu_e$ ,  $\bar{\nu}_e$  events were quite consistent

with no-oscillation model, there was a significant deficit of  $\nu_\mu, \bar{\nu}_\mu$  events caused by neutrinos coming from underneath. The explanation is that  $\nu_\mu$  and  $\bar{\nu}_\mu$  propagating from greater distances (other side of Earth) had more time to oscillate to a different flavour (mainly  $\nu_\tau, \bar{\nu}_\tau$ ) than those ones coming from above with the same energy.

As in case of solar neutrinos, it can be written in the two neutrino framework [1]

$$P_{\mu\mu}(L/E) = P_{\bar{\mu}\bar{\mu}}(L/E) = 1 - \sin^2(2\theta_{atm}) \sin^2\left(\frac{\Delta m_{atm}^2 L}{4E\hbar c}\right) \quad (1.18)$$

Experiments with atmospheric neutrinos were later overcome by accelerator experiments (K2K, T2K, MINOS) indicating that  $\theta_{23}$  is close to  $45^\circ$  so that  $\sin^2 2\theta_{23} \approx 1$ . That implies nearly maximal mixing between  $\nu_\mu$  ( $\bar{\nu}_\mu$ ) and  $\nu_\tau$  ( $\bar{\nu}_\tau$ ).

### 1.4.3 Measurement of $\theta_{13}$

Until recently, it was only known that the last mixing angle  $\theta_{13}$  is small, if not even zero. Fortunately, experiments with reactor  $\bar{\nu}_e$  (Daya Bay, Double Chooz, RENO) provided us with compelling evidence of a nonzero value of  $\theta_{13}$  in recent years ( $\theta_{13} \approx 9^\circ$ ).

The fact that  $\theta_{13}$  is relatively large is very important because it is a necessary condition of possible CP and T violation in neutrino oscillations.

### 1.4.4 Mass hierarchy and flavour content

Since only absolute value of  $\Delta m_{atm}^2$  ( $\Delta m_{31}^2, \Delta m_{32}^2$ ) is known, the question of neutrino mass hierarchy remains open. The mass eigenstate  $\nu_3$  can be either the state with the highest mass (such a scheme is called *normal hierarchy*) or the lowest mass (*inverted hierarchy*).

Unlike the mixing angles, the value of the CP violating phase  $\delta$  is still unknown however, it is a subject to intense research that will hopefully deliver results in the near future.

Putting our current knowledge together, the fractional flavour content in each neutrino mass eigenstate can be calculated. These flavour contents are drawn in Fig. 1.1, along with the two possible mass hierarchies. Besides, the flavour content is varied for  $\cos \delta \in [-1, 1]$  there. Exchange  $\delta \leftrightarrow -\delta$  does not affect it.



## 2. CP and T violation in neutrino oscillations

As it was said in the previous chapter, CP violation and connected T violation potentially observable in neutrino oscillations are caused by the  $\delta$  phase in the PMNS matrix. If all elements in the PMNS matrix were real, there would be no CP violation in neutrino oscillations.

### 2.1 Effect on oscillation probabilities

Let us focus on how the  $\delta$  phase actually affects oscillation probabilities. The most direct approach is to compare  $P_{\alpha\beta}$  with  $P_{\alpha\bar{\beta}}$  (CP violation) or with  $P_{\beta\alpha}$  (T violation):

$$\Delta P_{\alpha\beta}^{CP} \equiv P_{\alpha\beta} - P_{\alpha\bar{\beta}} \quad \Delta P_{\alpha\beta}^T \equiv P_{\alpha\beta} - P_{\beta\alpha} \quad (2.1)$$

Using CPT-symmetry we get:

$$\begin{aligned} 0 = \Delta P_{\alpha\beta}^{CPT} &\equiv P_{\alpha\beta} - P_{\bar{\beta}\alpha} = P_{\alpha\beta} - P_{\beta\alpha} + P_{\beta\alpha} - P_{\bar{\beta}\alpha} = \\ &= P_{\alpha\beta} - P_{\beta\alpha} - (P_{\alpha\beta} - P_{\alpha\bar{\beta}}) = \Delta P_{\alpha\beta}^T - \Delta P_{\alpha\beta}^{CP} = 0 \end{aligned} \quad (2.2)$$

This way we get  $\Delta P_{\alpha\beta}^{CP} = \Delta P_{\alpha\beta}^T$ . Furthermore [2],  $\Delta P^{CP} \equiv \Delta P_{e\mu}^{CP} = \Delta P_{\mu\tau}^{CP} = \Delta P_{\tau e}^{CP} = -\Delta P_{\mu e}^{CP} = \Delta P_{\tau\mu}^{CP} = \Delta P_{e\tau}^{CP}$ . The probability  $\Delta P^{CP}$  can be evaluated from (1.12) using standard parametrization of the PMNS matrix [1, 2]:

$$\begin{aligned} \Delta P^{CP} &= 2 \sum_{i<j} \text{Im}[U_{\alpha i}^* U_{\beta i} U_{\alpha j} U_{\beta j}^*] \sin\left(\frac{\Delta m_{ij}^2 L}{2E\hbar c}\right) = \\ &= -4 \sin(\delta) s_{12} c_{12} s_{23} c_{23} s_{13} c_{13}^2 \left[ \sin\left(\frac{\Delta m_{12}^2 L}{4E\hbar c}\right) + \sin\left(\frac{\Delta m_{23}^2 L}{4E\hbar c}\right) + \sin\left(\frac{\Delta m_{31}^2 L}{4E\hbar c}\right) \right] = \\ &= -2 \sin(\delta) \cos(\theta_{13}) \sin(2\theta_{12}) \sin(2\theta_{13}) \sin(2\theta_{23}) \cdot \\ &\quad \cdot \sin\left(\frac{\Delta m_{12}^2 L}{4E\hbar c}\right) \sin\left(\frac{\Delta m_{23}^2 L}{4E\hbar c}\right) \sin\left(\frac{\Delta m_{13}^2 L}{4E\hbar c}\right) \end{aligned} \quad (2.3)$$

From Eq. (2.3) follows that  $\Delta P^{CP} \neq 0$  only if  $\Delta m_{ij}^2 \neq 0 \quad \forall i \neq j$  and  $\theta_{12}, \theta_{13}, \theta_{23} \neq 0^\circ, 90^\circ$ . The magnitude of  $\Delta P^{CP}$  is determined then by  $\delta$ .

The probability  $\Delta P^{CP}$  derived in Eq. (2.3) is drawn in Fig. 2.1 for  $\delta = 0, \pi/2, \pi, 3\pi/2$ . It has oscillatory behaviour dependant on  $\Delta m_{ij}^2$  and  $L/E$ , similarly to the normal oscillation probabilities. The maximal possible amplitude of those oscillations is  $2 \sin(\delta) \cos(\theta_{13}) \sin(2\theta_{12}) \sin(2\theta_{13}) \sin(2\theta_{23}) \approx 0.56$  for current values of mixing angles and  $\sin \delta = \pm 1$ .

In order to maximize sensitivity to  $\Delta P^{CP}$ , the value of  $L/E$  in an experiment should correspond to a peak of the continuous line in Fig. 2.1. The height of those peaks increases with  $L/E$  (up to  $L/E \approx 10\,000 \text{ km/GeV}$ ) making CP violation more significant. Nevertheless, for the fixed neutrino energy the increase in  $L/E$  means an adequate increase of the length of the experiment baseline, which might bring difficulties.

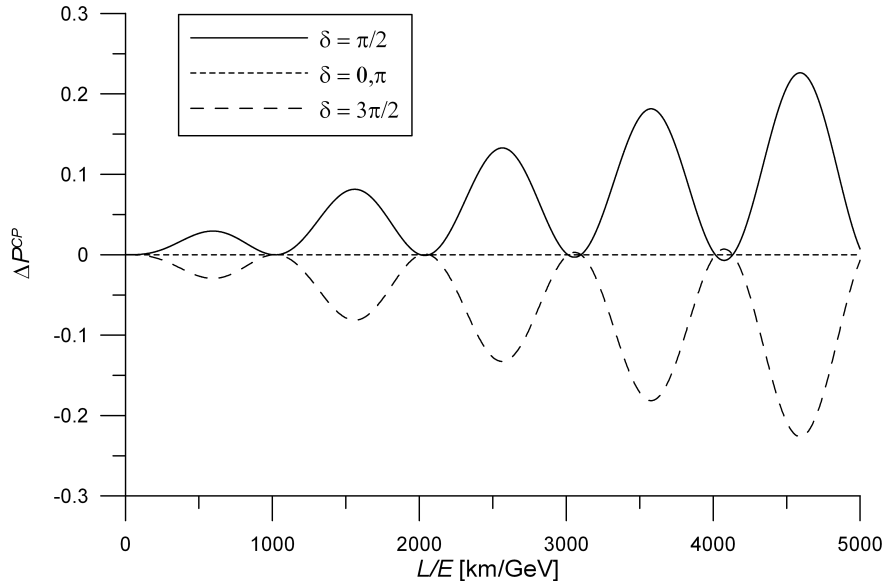


Figure 2.1: The CP violating probability  $\Delta P^{CP}$  as a function of  $L/E$  in vacuum. On this scale the approximation  $\sin\left(\frac{\Delta m_{23}^2 L}{4E\hbar c}\right) \sin\left(\frac{\Delta m_{13}^2 L}{4E\hbar c}\right) \cong \sin^2\left(\frac{\Delta m_{atm}^2 L}{4E\hbar c}\right)$  is valid. That makes the  $\Delta P^{CP}$  function  $(\sin^2 x)$ -like slowly moderated by the  $\sin\left(\frac{\Delta m_{12}^2 L}{4E\hbar c}\right)$  term. However, the difference between  $\Delta m_{13}^2$  and  $\Delta m_{23}^2$  manifests itself on a greater scale (for greater values of  $L/E$ ).

## 2.2 Measurement

Currently, there are two possible approaches to the measurement of CP violation in neutrino oscillations. The first is the comparison of  $P_{\mu e}$  and  $P_{\bar{\mu} \bar{e}}$  (as it is explained above). The second is the comparison of  $P_{\mu e}$  (or  $P_{\bar{\mu} \bar{e}}$ ) and  $P_{ee} = P_{\bar{e} \bar{e}}$ .

The reason why our options are so limited is that the  $\nu_\mu \rightarrow \nu_e$  and  $\bar{\nu}_\mu \rightarrow \bar{\nu}_e$  channels are currently the only appearance channels used in the search of CP violation in neutrino oscillations. The measurement of those channels is provided by two experiments, namely the T2K experiment with the mean neutrino energy of 0.63 GeV and the baseline of 295 km and the NO $\nu$ A experiment with the mean neutrino energy of 2.0 GeV and the baseline of 810 km.

Now we shall calculate threshold energies of neutrino-nucleon charge current quasi-elastic interactions in order to show why other appearance channels (especially  $\nu_e \rightarrow \nu_\mu$  and  $\bar{\nu}_e \rightarrow \bar{\nu}_\mu$ ) are not currently used.

### 2.2.1 Threshold energies

Let us now consider the simplest case of the neutrino charge current quasi-elastic interaction in which a neutrino interacts with a single nucleon, i.e. the neutrino with the neutron and the antineutrino with the proton:

$$\nu_e/\nu_\mu/\nu_\tau + n \longrightarrow e^-/\mu^-/\tau^- + p \quad \bar{\nu}_e/\bar{\nu}_\mu/\bar{\nu}_\tau + p \longrightarrow e^+/\mu^+/\tau^+ + n \quad (2.4)$$

We can calculate the threshold energy  $E_{thr}$  from energy and momentum conservation laws, in other words  $E_{thr}$  is the neutrino (antineutrino) energy for which

the proton (neutron) and the charged lepton are produced motionless in CMS:

$$E_{thr} = \frac{(m_p + m_\alpha)^2 - m_n^2}{2m_n} \text{ for } \nu_\alpha \quad E_{thr} = \frac{(m_n + m_\alpha)^2 - m_p^2}{2m_p} \text{ for } \bar{\nu}_\alpha \quad (2.5)$$

where  $m_p$ ,  $m_n$  and  $m_\alpha$  denote the mass of the proton, neutron and lepton  $\alpha \in \{e, \mu, \tau\}$  respectively. The masses of neutrinos were neglected.

Those threshold energies can be easily evaluated - see Tab. 2.1. However, actual energies necessary for the (anti)neutrino (flavour determining) detection in real experiments would be probably higher.

$\nu_e$	no thr.	$\bar{\nu}_e$	1.8 MeV
$\nu_\mu$	110.2 MeV	$\bar{\nu}_\mu$	113.0 MeV
$\nu_\tau$	3453.2 MeV	$\bar{\nu}_\tau$	3463.2 MeV

Table 2.1: Threshold energies for charge current quasi-elastic interactions of (anti)neutrino with neutron (proton) according to Eq. (2.5). Masses of particles were taken from [6].

As we can see in Tab. 2.1, both  $\nu_\tau$  and  $\bar{\nu}_\tau$  must have the energy of nearly 3.5 GeV to be able to interact in such a way. If we want to observe  $\nu_\tau$  and  $\bar{\nu}_\tau$ , we need a source of neutrinos with adequate energies. Moreover, the mean life of  $291 \cdot 10^{-15}$  s [6] makes  $\tau$  quite difficult to detect (e.g. in the DONUT experiment, which provided the first compelling evidence of the  $\nu_\tau$  existence, the technique of nuclear emulsions was revived for the detection of  $\nu_\tau$  [9]).  $\nu_\tau$  and  $\bar{\nu}_\tau$  can interact via the neutral current as well, but in such a case the neutrino flavour cannot be determined.

Another nuisance which makes the usage of  $\nu_\tau$  and  $\bar{\nu}_\tau$  channels very limited is the fact that the production of  $\nu_\tau$  and  $\bar{\nu}_\tau$  is much more difficult than in the case of  $\nu_\mu$  and  $\bar{\nu}_\mu$  or  $\nu_e$  and  $\bar{\nu}_e$ , considering that a well-defined beam is needed for precision measurements.

Let us now focus on  $\nu_\mu$  and  $\bar{\nu}_\mu$ . We can see in Tab. 2.1 that  $\nu_\mu$  ( $\bar{\nu}_\mu$ ) must have energy over 110 MeV (113 MeV) to be able to interact in the described way. That naturally sets constraints on the usage of  $\nu_e \rightarrow \nu_\mu$  and  $\bar{\nu}_e \rightarrow \bar{\nu}_\mu$  channels for neutrino oscillation experiments.  $\nu_e$  or  $\bar{\nu}_e$  with energies of at least hundreds of MeV or several GeV are needed.

When talking about man-made sources of  $\nu_e$  and  $\bar{\nu}_e$ , nuclear reactors are currently the only source of  $\bar{\nu}_e$  for oscillation experiments (KamLAND, Daya Bay, Double Chooz, RENO), but those  $\bar{\nu}_e$ s have energy of only few MeV, far below the threshold energy for  $\mu^+$  creation. Regarding using accelerators, only  $\nu_\mu$  and  $\bar{\nu}_\mu$  are produced for oscillation experiments nowadays. They come from  $\pi^+$  and  $\pi^-$  decays for which the production of  $\nu_e$  or  $\bar{\nu}_e$  is strongly suppressed. Nevertheless, there are several concepts of  $\nu_e$  and  $\bar{\nu}_e$  sources with sufficient energies:

- *Beta beams*[10]: This concept supposes to use beta decays. Beta decays are a source of  $\bar{\nu}_e$  ( $\beta^-$  decay, this is where the reactor  $\bar{\nu}_e$ s come from) or  $\nu_e$  ( $\beta^+$  decay), but neutrino energy usually does not exceed several MeV. However, this problem may be partially solved by accelerating decaying

nuclei. That increases neutrino energy and collimates emitted neutrinos in a narrow beam, better suited for oscillation experiments. The spectrum of neutrino energy is continuous (because the beta decay is a three-body decay) and very well known. However, in case of an electron capture (i.e. nucleus decays by capturing an electron from its own electron cloud) monochromatic  $\nu_e$ s are emitted. So, the later alternative requires the nucleus having at least one electron present in its atomic orbital to be accelerated.

- *The neutrino factory*[11, 12, 13]: The other possibility is to use muons as a source of neutrinos. Namely  $\mu^-$  as a source of  $\nu_\mu$  and  $\bar{\nu}_e$  (at the same time) or  $\mu^+$  as source of  $\bar{\nu}_\mu$  and  $\nu_e$  (at the same time). As in the previous case, neutrinos emitted when muons decay at rest do not have sufficient energy (even though the energy exceeds 50 MeV which is more than in the beta decay case). That can be solved by boosting muons to the convenient momentum and then storing them in an accelerator ring with extended straight sections. Neutrinos and antineutrinos emitted in decays of muons in the straight sections create a narrow beam which energy spectrum is precisely known. Such a scenario is already considered as the nuSTORM facility [12, 13].

## 2.2.2 Neutrino-nucleon scattering cross section

The chance to investigate the  $\nu_e \rightarrow \nu_\mu$  and  $\bar{\nu}_e \rightarrow \bar{\nu}_\mu$  channels is not the only benefit of the facility producing electron (anti)neutrinos with sufficient energies. Even experiments focusing on  $\nu_\mu \rightarrow \nu_e$  and  $\bar{\nu}_\mu \rightarrow \bar{\nu}_e$  channels are dependant on our knowledge of the electron (anti)neutrino-nucleon scattering cross section for which there is essentially no data. For that reason extrapolations from muon (anti)neutrino cross sections are made which brings considerable uncertainties. Moreover, even for muon (anti)neutrinos with energies of hundreds of MeV or few GeV the knowledge of the scattering cross section is not very precise (uncertainties are typically 10 - 40% [15]) because cross section measurements in this region are sparse. As we can see in Fig. 2.2, the situation for  $\bar{\nu}_\mu$  is worse than for  $\nu_\mu$ .

The nuSTORM facility may provide a neutrino beam (with precisely known flavour composition, energy spectrum and flux) not only for oscillation experiments, but also for crucial scattering cross section measurements, with a precision approaching 1% [12, 13].

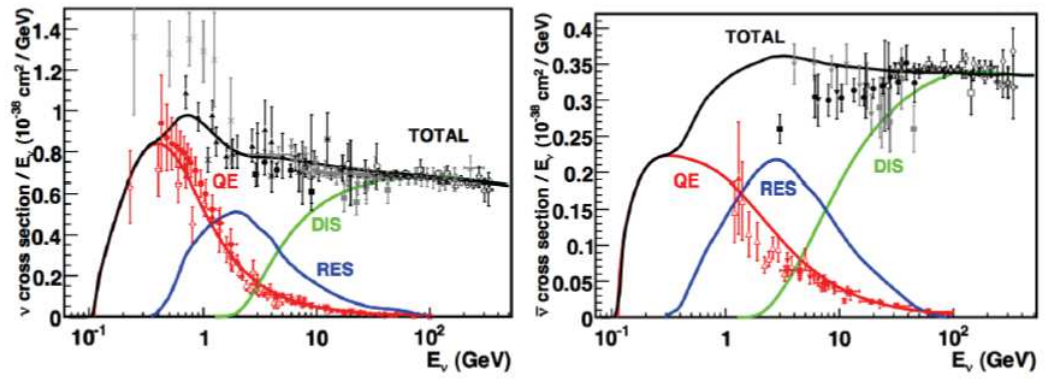


Figure 2.2: The muon neutrino-nucleon (left) and muon antineutrino-nucleon (right) charge current cross section: measured data and models described in [14]. Contributing processes are: quasi-elastic scattering (QE, red), resonance production (RES, blue) and deep inelastic scattering (DIS, green). Black colour denotes the total cross section. This figure was taken from [15].

### 3. Sterile neutrinos

This chapter is based on the information from [12, 13, 16].

Although most of neutrino oscillation experiments can be explained within the three active neutrino framework, there are several exceptions suggesting that such a model may not be sufficient. One way how to cope with these anomalies is to add one or more sterile neutrino species. Sterile neutrinos do not interact weakly and arise naturally in many extensions of the Standard Model.

The first hint for the possible existence of sterile neutrinos came from the result of the LSND collaboration which investigated the  $\bar{\nu}_\mu \rightarrow \bar{\nu}_e$  oscillation channel by using  $\bar{\nu}_\mu$ s from decays of  $\pi^+$  at rest and subsequent decays of  $\mu^+$ . The baseline was  $\approx 30$  m. The excess of  $\bar{\nu}_e$  events above background with the significance of  $3\sigma$  was reported. The explanation is that the oscillation through an intermediate sterile state  $\bar{\nu}_s$  with mass-squared splitting  $\Delta m^2 \gtrsim 0.1\text{eV}^2$  relative to active neutrinos happened.

The second anomaly occurred in the MiniBooNE experiment, which was designed to verify LSND results. It used  $\pi^+$  and  $\pi^-$  beams producing  $\nu_\mu$  and  $\bar{\nu}_\mu$  respectively. The excess in both  $\bar{\nu}_\mu \rightarrow \bar{\nu}_e$  and  $\nu_\mu \rightarrow \nu_e$  channels with significance above  $3\sigma$  was confirmed.

A third hint indicating existence of sterile neutrinos is the so-called *reactor antineutrino anomaly*. When in 2011 new calculation of the reactor  $\bar{\nu}_e$  flux was published, it showed that the flux is about 3% higher than it had been previously supposed. The implication is that the short-baseline experiments measuring reactor  $\bar{\nu}_e$  have observed significant deficit of  $\bar{\nu}_e$ . One explanation is that  $\bar{\nu}_e$  disappeared via the  $\bar{\nu}_e \rightarrow \bar{\nu}_s$  channel.

Another anomaly is the Gallium anomaly. The amount of  $\nu_e$  from artificial sources  $^{51}\text{Cr}$  and  $^{37}\text{Ar}$  measured in the experiments performed to calibrate SAGE and GALLEX detectors was lower than expected. The explanation based on short-baseline oscillations via sterile neutrinos may be applied in this case.

All those hints give us motivation to search for neutrino oscillations driven by  $\Delta m^2 \simeq 0.1 - 1\text{eV}^2$  to either verify or rule out the possible existence of light sterile neutrinos (which mix with active neutrinos). Such a measurement might be provided for example by the nuSTORM facility.

# 4. Muons as a source of neutrinos

## 4.1 Neutrino factory

The idea of using muons as a source of neutrinos dates back to 1970-s. This concept is now known as the *neutrino factory*.

Although many specifications may vary, the basic scheme is always the same. It starts with accelerating protons up to energies of tenths or hundreds of GeV. These protons are aimed to a target to produce pions that decay mostly into muons and muon (anti)neutrinos:  $\pi^+ \rightarrow \mu^+ + \nu_\mu$  or  $\pi^- \rightarrow \mu^- + \bar{\nu}_\mu$ . Muons are placed into a storage ring which consists of several long straight sections and arcs. Straight sections are pointed towards detectors so that neutrinos produced in muon decays (dominant muon decay:  $\mu^+ \rightarrow \bar{\nu}_\mu + \nu_e + e^+$  or  $\mu^- \rightarrow \nu_\mu + \bar{\nu}_e + e^-$ ) may be observed in various short- or long-baseline experiments. While this scheme applies for neutrino factory concepts in general, specific attributes may vary. The muon momentum is usually considered to be 1 - 50 GeV, the way of collecting muons from decaying pions differs quite a lot etc. The concept we will focus on is called nuSTORM ( $\nu$ STORM).

To start with we will make a brief comparison between pions and muons from the perspective of a neutrino source. Since all the artificial sources of high energy neutrinos use pion decays (e.g. T2K or NuMI at Fermilab providing the neutrino beam for NO $\nu$ A, MINOS+ and MINER $\nu$ A), it is quite reasonable to pose a question what improvement may be achieved by using muons instead of pions [11]:

- As it was mentioned in the previous chapter, neutrino beams based on pion decays can provide neither  $\nu_e$  nor  $\bar{\nu}_e$  beam (suitable for experiments) while the beams based on muon decays provide that.
- Although the beam based on pion decays consists mostly of  $\nu_\mu$  or  $\bar{\nu}_\mu$ , small contamination with  $\nu_e$  or  $\bar{\nu}_e$  (originating mostly in  $K^\pm$  decays) is inevitable. Moreover, even small fraction of  $\nu_\tau$  or  $\bar{\nu}_\tau$  may be present (originating mostly in  $D_s^\pm$  decays) if the energy of protons on target is high enough. Such a contamination is a nuisance for most oscillation experiments. On contrary, stored muons produce the flux of the precisely known flavour content - 50% of  $\bar{\nu}_\mu + 50\%$  of  $\nu_e$  for  $\mu^+$  or 50% of  $\nu_\mu$  and 50% of  $\bar{\nu}_e +$  for  $\mu^-$ . Nevertheless, the detector using such a beam must be able to distinguish the charge of leptons produced by (anti)neutrino interactions in order to differentiate between neutrino and antineutrino channels.
- The muon storage ring concept allows the (anti)neutrino flux to be measured with a precision of 1% which is better than the precision of currently used beams based on pion decays.

On the other hand, it is much easier to create a neutrino beam based on pion decays than the one based on muon decays.

## 4.2 nuSTORM facility

The nuSTORM (neutrinos from STORed Muons) facility [12, 13] is one of the considered implementations of the neutrino factory concept. It is projected to operate with muons of momenta 3.8 GeV. Because of requirements on infrastructure of proton-accelerator laboratories only CERN and FNAL qualify as possible locations.

The main goals of the nuSTORM facility are [12], [13]:

- To resolve the question of sterile neutrinos with excellent sensitivity;
- To make precise measurement of electron and muon (anti)neutrino scattering cross sections on nuclei;
- To provide a neutrino beam of a precisely known flavour content and energy spectrum for detector studies and neutrino experiments;
- To provide a technology (the  $\mu$  decay ring) test demonstration and  $\mu$  diagnostics test bed.

The basic scheme of the nuSTORM facility can be seen in Fig. 4.1. Protons accelerated to 100 GeV (CERN) or 60 GeV (FNAL) hit the target and produce pions, kaons etc. The pions with momentum of approximately 5 GeV are focused by a collection element (horn or lithium lens), transported and injected to a storage ring that consists of two straight sections and two arcs. The pions that decay within the first straight (about 40%, the rest is dumped into an absorber) produce muons and a fraction of those muons is then stored in the ring so they eventually decay into desired neutrinos.

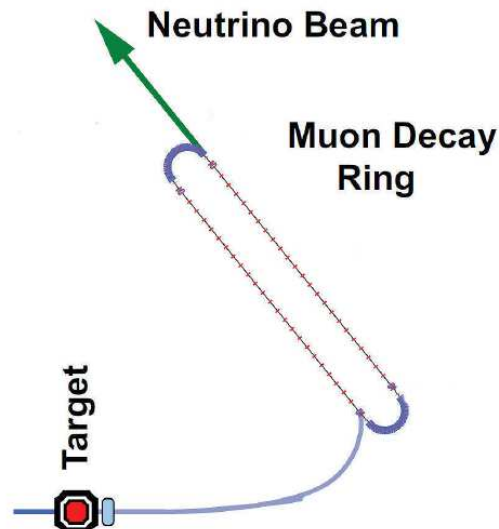


Figure 4.1: The basic scheme of the nuSTORM facility. This figure was taken from [12].

The muon storage ring is designed to circulate muons with a central momentum of 3.8 GeV and a momentum spread of 10%. It has a racetrack shape with the total circumference of 350 m consisting of two 150 m straights and two 25 m

arcs. It is expected that  $\approx 10^{21}$  protons on target will lead to  $\approx 10^{18}$  useful muon decays.

Basically, two detectors are planned - the 100 Ton near detector 50 m from the storage ring and the 1.6 kTon far detector approximately 1.5 km from the storage ring. Iron and scintillator sampling calorimeters similar to MINOS (SuperBIND - see [12] or [13] for more information) will be used. A toroidal magnetic field will allow to distinguish the charge of observed particles. The main purpose of the near detector is to measure characteristics of the neutrino beam before oscillations evolve. The far detector will study neutrino oscillation physics.

That is the nuSTORM facility at large. Now we shall look at the muon decay in more detail.

### 4.3 Decay of muon at rest

There are the two possibilities -  $\mu^+$  and  $\mu^-$  decay. We will focus on the later. Nevertheless, it should be said that the case of  $\mu^+$  decay is analogous. The dominant (over 98% [6]) decay of  $\mu^-$  is:

$$\mu^- \longrightarrow \nu_\mu + \bar{\nu}_e + e^- \quad (4.1)$$

The aim of this section is to calculate the differential decay rate  $\frac{d\Gamma}{dE_\nu}$  which is proportional to the probability density  $\frac{dP}{dE_\nu}$  of emission of  $\nu_\mu$  with energy  $E_\nu$  in the decay of  $\mu^-$  at rest and to calculate the analogous expression for  $\bar{\nu}_e$ .

In general we can use the equation for a decay rate in a three-body decay [1]:

$$d\Gamma = \frac{1}{2M} |\mathcal{M}|^2 d\Phi_3 \quad (4.2)$$

where  $M$  is the mass of the decaying particle,  $\mathcal{M}$  is the matrix element for the particular decay and  $d\Phi_3$  is an element of a three-body phase space. In the case of an unpolarized  $\mu^-$  decay, the matrix element  $\mathcal{M}$  is [17]:

$$|\mathcal{M}|^2 = 64G_F^2 (p \cdot k') (p' \cdot k) \quad (4.3)$$

where  $G_F$  is the Fermi coupling constant and  $p'$ ,  $p$ ,  $k'$  and  $k$  denote four-momenta of  $\mu^-$ ,  $e^-$ ,  $\nu_\mu$  and  $\bar{\nu}_e$  respectively.

The element of the three-body phase space  $d\Phi_3$  can be rewritten in the form:

$$d\Phi_3(M, m_1, m_2, m_3) = d\Phi_2(M, m_{12}, m_3) d\Phi_2(m_{12}, m_1, m_2) \frac{dm_{12}^2}{2\pi} \quad (4.4)$$

where  $m_1$ ,  $m_2$  and  $m_3$  are masses of emitted particles,  $m_{12}$  is the invariant mass of particles 1 and 2 and finally the element of a two-body phase space is:

$$d\Phi_2(M, m_1, m_2) = \frac{1}{16\pi^2} \frac{p_{cms}}{M} d\cos\theta d\phi \quad (4.5)$$

where  $p_{cms}$  is the absolute value of the three-momentum of emitted particles in the CMS of the decaying particle and angles  $\theta$  and  $\phi$  describe the direction of emitted particles.

In our case, we consider unpolarized  $\mu^-$  of the mass  $M_\mu$  and the four-momentum  $p'$  decaying into  $\nu_\mu$ ,  $\bar{\nu}_e$  and  $e^-$  of four-momenta  $k'$ ,  $k$  and  $p$  respectively (in the rest

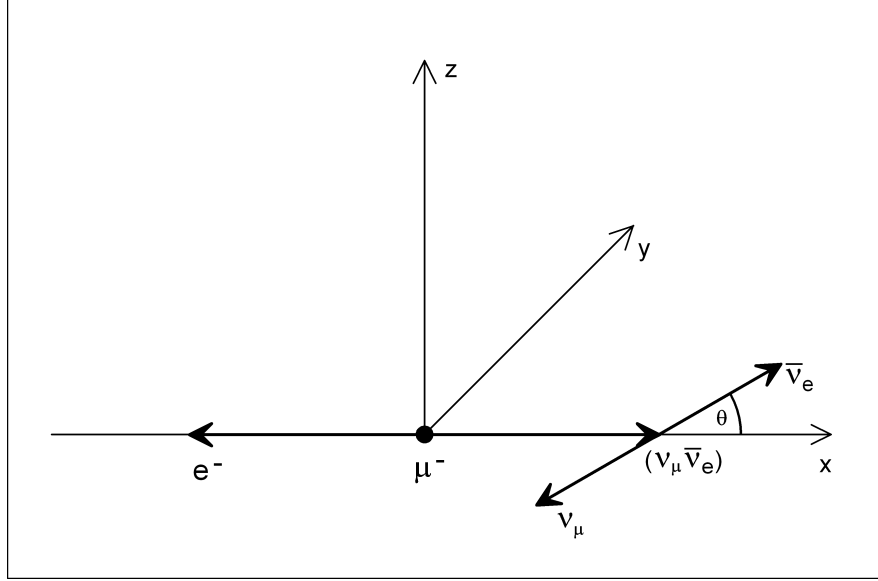


Figure 4.2: Scheme of the muon decay

frame of  $\mu^-$ ). We neglect masses of emitted particles because they are very low compared to the mass of the parent particle  $\mu^-$  ( $m_e/M_\mu \approx 5 \cdot 10^{-3}$  and neutrino masses are much lower).

As we deal with an unpolarized  $\mu^-$ , there is no preferred direction of the emission of an  $e^-$  (or  $\nu_\mu, \bar{\nu}_e$ ). In order to calculate the matrix element  $|\mathcal{M}|^2$  we can choose the scheme drawn in Fig. 4.2. The  $(\nu_\mu \bar{\nu}_e)$  pair of invariant mass  $m_{12}$  is emitted along the x-axis (the  $e^-$  is emitted in the opposite direction then). The angle between the  $\bar{\nu}_e$  momentum in the CMS of the  $(\nu_\mu \bar{\nu}_e)$  pair and the direction of a flight of the  $(\nu_\mu \bar{\nu}_e)$  pair in the  $\mu^-$  rest frame (along x-axis) is  $\theta$ . The result does not depend on the actual choice of axes (it depends only on  $m_{12}$  and  $\theta$ ), but this choice makes consequent calculations easier. Using this scheme we can calculate  $p', k', k$  and  $p$  from kinematics of a two body decay. For  $\mu^-$  and  $e^-$  we get pretty straightforward:

$$p' = (M_\mu, 0, 0, 0) \quad (4.6)$$

$$p = \left( \frac{M_\mu^2 - m_{12}^2}{2M_\mu}, -\frac{M_\mu^2 - m_{12}^2}{2M_\mu}, 0, 0 \right) \quad (4.7)$$

However,  $\nu_\mu$  and  $\bar{\nu}_e$  four-momenta are easily defined only in the CMS of the  $(\nu_\mu \bar{\nu}_e)$  pair (denoted  $k_0$  and  $k'_0$ ):

$$k'_0 = \left( \frac{m_{12}}{2}, -\frac{m_{12}}{2} \cos \theta, -\frac{m_{12}}{2} \sin \theta \cos \phi, -\frac{m_{12}}{2} \sin \theta \sin \phi \right) \quad (4.8)$$

$$k_0 = \left( \frac{m_{12}}{2}, \frac{m_{12}}{2} \cos \theta, \frac{m_{12}}{2} \sin \theta \cos \phi, \frac{m_{12}}{2} \sin \theta \sin \phi \right) \quad (4.9)$$

To find out  $k'$  and  $k$  we need to use the Lorentz transformation along the x-axis with relativistic factors  $\gamma = \frac{M_\mu^2 + m_{12}^2}{2M_\mu m_{12}}$  and  $\beta = \frac{M_\mu^2 - m_{12}^2}{M_\mu^2 + m_{12}^2}$ . The transformation can be written in the matrix form:

$$k' = \begin{pmatrix} \gamma & \beta\gamma & 0 & 0 \\ \beta\gamma & \gamma & 0 & 0 \\ 0 & 0 & 1 & 0 \\ 0 & 0 & 0 & 1 \end{pmatrix} k'_0 \quad (4.10)$$

The same applies for  $k_0$ . Using that we obtain:

$$k' = \left( \frac{1}{4M_\mu}(M_\mu^2 + m_{12}^2 - (M_\mu^2 - m_{12}^2) \cos \theta), \right. \\ \left. \frac{1}{4M_\mu}(M_\mu^2 - m_{12}^2 - (M_\mu^2 + m_{12}^2) \cos \theta), k'_{0y}, k'_{0z} \right) \quad (4.11)$$

$$k = \left( \frac{1}{4M_\mu}(M_\mu^2 + m_{12}^2 + (M_\mu^2 - m_{12}^2) \cos \theta), \right. \\ \left. \frac{1}{4M_\mu}(M_\mu^2 - m_{12}^2 + (M_\mu^2 + m_{12}^2) \cos \theta), k'_{0y}, k'_{0z} \right) \quad (4.12)$$

Putting the expressions for  $p'$ ,  $p$ ,  $k'$ ,  $k$  to Eq. (4.2) and integrating over all angles except for  $\cos \theta$  (because the only angle which the decay rate depends on is  $\theta$ ; integrating over the rest angles is trivial) we get:

$$d\Gamma = \frac{G_F^2}{128\pi^3 M_\mu^3} (1 - \cos \theta) (M_\mu^2 - m_{12}^2)^2 (M_\mu^2 + m_{12}^2 + (M_\mu^2 - m_{12}^2) \cos \theta) d\cos \theta dm_{12}^2 \quad (4.13)$$

To obtain desired  $\frac{d\Gamma}{dE_\nu}$  we must transform variables  $(\cos \theta, m_{12}^2) \rightarrow (\cos \theta, E_\nu)$  where  $E_\nu = \frac{1}{4M_\mu}(M_\mu^2 + m_{12}^2 - (M_\mu^2 - m_{12}^2) \cos \theta)$  is the energy of  $\nu_\mu$ ;  $E_\nu \in [0, \frac{M_\mu}{2}]$  and for a fixed energy  $\cos \theta \in [1 - \frac{4E_\nu}{M_\mu}, 1]$ . The Jacobian of this transformation is  $\frac{4M_\mu}{1 + \cos \theta}$ . Applying these alterations on the Eq. (4.13) leads to equation:

$$d\Gamma = G_F^2 \frac{M_\mu}{2\pi^3} \frac{1 - \cos \theta}{(1 + \cos \theta)^4} (M_\mu \cos \theta + E_\nu(1 - \cos \theta)) d\cos \theta dE_\nu \quad (4.14)$$

Now we may integrate this equation over  $\cos \theta$  and divide it by  $dE_\nu$  to obtain the final formula for  $\nu_\mu$ :

$$\frac{d\Gamma}{dE_\nu} = G_F^2 \frac{M_\mu}{12\pi^3} E_\nu^2 (3M_\mu - 4E_\nu) \quad (4.15)$$

In the case of  $\frac{d\Gamma}{dE_{\bar{\nu}}}$  we shall proceed in an analogous way. The expression for the energy of  $\bar{\nu}_e$  is  $E_{\bar{\nu}} = \frac{1}{4M_\mu}(M_\mu^2 + m_{12}^2 + (M_\mu^2 - m_{12}^2) \cos \theta)$ , the Jacobian and possible values of  $E_{\bar{\nu}}$  remain the same, except for  $\cos \theta \in [-1, \frac{4E_{\bar{\nu}}}{M_\mu} - 1]$ . In analogy to Eq. (4.14) we get:

$$d\Gamma = G_F^2 \frac{M_\mu}{2\pi^3} \frac{1}{(1 - \cos \theta)^2} E_{\bar{\nu}} (M_\mu - 2E_{\bar{\nu}})^2 d\cos \theta dE_{\bar{\nu}} \quad (4.16)$$

As in the previous case, we shall integrate this equation over  $\cos \theta$  and divide it by  $dE_{\bar{\nu}}$  to obtain the final formula for  $\bar{\nu}_e$ :

$$\frac{d\Gamma}{dE_{\bar{\nu}}} = G_F^2 \frac{M_\mu}{2\pi^3} E_{\bar{\nu}}^2 (M_\mu - 2E_{\bar{\nu}}) \quad (4.17)$$

In order to check the results we may integrate Eq. (4.15) over  $E_\nu$  or Eq. (4.17) over  $E_{\bar{\nu}}$  to get:

$$\Gamma = G_F^2 \frac{M_\mu^5}{192\pi^3} \quad (4.18)$$

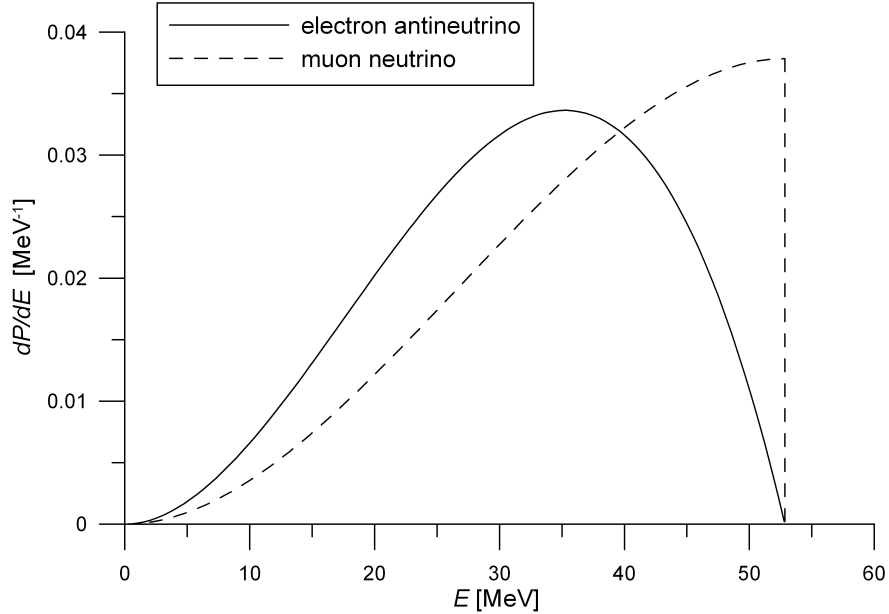


Figure 4.3: Energy distribution  $\frac{dP}{dE}$  of  $\nu_\mu$  and  $\bar{\nu}_e$  emitted in the decay of a  $\mu^-$  at rest

If we evaluate  $\Gamma$  using  $G_F = 1.166 \cdot 10^{-5} \text{ GeV}^{-2}$  and  $M_\mu = 0.1056 \text{ GeV}$  [6] we get  $\Gamma = 3.0 \cdot 10^{-19} \text{ GeV}$  which corresponds to the mean lifetime of  $2.2 \cdot 10^{-6} \text{ s}$ . That is the correct value according to [6].

Besides, we can easily derive  $\frac{dP}{dE_\nu} \propto \frac{d\Gamma}{dE_\nu}$  and  $\frac{dP}{dE_{\bar{\nu}}} \propto \frac{d\Gamma}{dE_{\bar{\nu}}}$ . All we have to do is to normalize the formulae (4.15) and (4.17) so that  $\int \frac{dP}{dE} dE = 1$ .

$$\frac{dP}{dE_\nu} = \frac{16}{M_\mu^4} E_\nu^2 (3M_\mu - 4E_\nu) \quad (4.19)$$

$$\frac{dP}{dE_{\bar{\nu}}} = \frac{96}{M_\mu^4} E_{\bar{\nu}}^2 (M_\mu - 2E_{\bar{\nu}}) \quad (4.20)$$

The distributions  $\frac{dP}{dE_\nu}$  and  $\frac{dP}{dE_{\bar{\nu}}}$  are drawn in Fig. 4.3. It has revealed that they differ quite a lot for  $\nu_\mu$  and  $\bar{\nu}_e$ . While for  $\nu_\mu$  the maximum of  $\frac{dP}{dE}$  is associated with  $E_{M\nu} = \frac{M_\mu}{2}$ , for  $\bar{\nu}_e$  it is  $E_{M\bar{\nu}} = \frac{M_\mu}{3}$ . The probability of emission of a  $\bar{\nu}_e$  with the energy approaching to  $\frac{M_\mu}{2}$  decreases to 0.

The reason for this discrepancy is the matrix element  $\mathcal{M}$  which reflects the specific character of weak interactions and is not symmetric under the exchange of  $\nu_\mu$  and  $\bar{\nu}_e$ . If we used  $|\mathcal{M}|^2 = 1$  instead,  $\frac{dP}{dE_\nu}$  and  $\frac{dP}{dE_{\bar{\nu}}}$  would be linear functions of  $E_\nu$  and  $E_{\bar{\nu}}$  respectively (and the same would apply for  $e^-$  as well).

## 4.4 Decay of muon in motion

In this section we shall look at the decay of a  $\mu^-$  in motion using results from the previous section.

Let us assume that we have a  $\mu^-$  that moves along x-axis with the momentum  $p_\mu$  (see Fig. 4.4 for the scheme), energy  $E_\mu = \sqrt{M_\mu^2 + p_\mu^2}$  and corresponding relativistic factors  $\gamma = E_\mu/M_\mu$  and  $\beta = p_\mu/E_\mu$ .

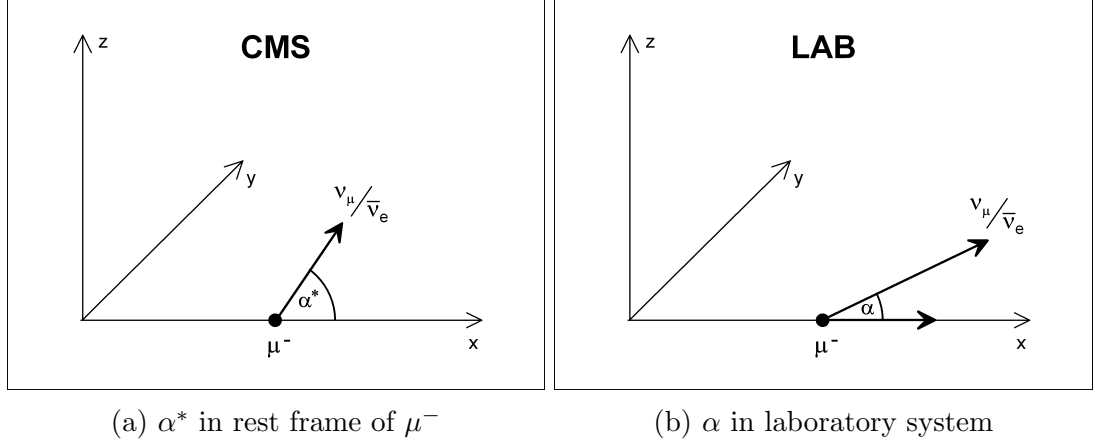


Figure 4.4: Scheme of decay of  $\mu^-$  in motion

However, what we know are  $\nu_\mu$  and  $\bar{\nu}_e$  energy distributions in the rest frame of the  $\mu^-$  (they are described in Eq. (4.15) and (4.17)). If  $\alpha^*$  denotes the angle between the  $\nu_\mu$  or  $\bar{\nu}_e$  momentum (calculations are analogous for  $\nu_\mu$  and  $\bar{\nu}_e$ ) and the x-axis in the rest frame of the  $\mu^-$ , formulae (4.15) and (4.17) can be altered:

$$d\Gamma = G_F^2 \frac{M_\mu}{24\pi^3} (E_\nu^*)^2 (3M_\mu - 4E_\nu^*) dE_\nu^* d\cos\alpha^* \quad (4.21)$$

$$d\Gamma = G_F^2 \frac{M_\mu}{4\pi^3} (E_\nu^*)^2 (M_\mu - 2E_\nu^*) dE_\nu^* d\cos\alpha^* \quad (4.22)$$

The formula (4.21) tells us what is the decay rate leading to the emission of  $\nu_\mu$  with the four-momentum  $p_\nu^*$  in the rest frame of  $\mu^-$ :

$$p_\nu^* = (E_\nu^*, E_\nu^* \cos\alpha^*, E_\nu^* \sin\alpha^* \cos\eta^*, E_\nu^* \sin\alpha^* \sin\eta^*) \quad (4.23)$$

where the angle  $\eta^*$  does not play any role in consequent calculations, only the first two components of  $p_\nu^*$  are important. Using the Lorentz transformation in the same way as in (4.10) we get the corresponding four-momentum in the laboratory system:

$$p_\nu = (\gamma E_\nu^* (1 + \beta \cos\alpha^*), \gamma E_\nu^* (\beta + \cos\alpha^*), p_{\nu y}^*, p_{\nu z}^*) \quad (4.24)$$

We can see that the  $\nu_\mu$  energy in laboratory frame is  $E_\nu = \gamma E_\nu^* (1 + \beta \cos\alpha^*)$  and the x-component of the  $\nu_\mu$  momentum is  $p_{\nu x} = \gamma E_\nu^* (\beta + \cos\alpha^*)$ . For the angle between the  $\nu_\mu$  momentum and the x-axis (which is the direction of flight of  $\mu^-$ ) the following equation applies:

$$\cos\alpha = \frac{p_{\nu x}}{E_\nu} = \frac{\beta + \cos\alpha^*}{1 + \beta \cos\alpha^*} \quad (4.25)$$

Since we have neglected masses of  $\nu_\mu$  and  $\bar{\nu}_e$ , the angle  $\alpha$  is not dependent on energy of  $\nu_\mu$  or  $\bar{\nu}_e$ . The relation for  $\alpha$  (4.25) can be inverted:

$$\cos\alpha^* = \frac{\cos\alpha - \beta}{1 - \beta \cos\alpha} \quad (4.26)$$

Besides, we can invert the relation for the energy as well:

$$E_\nu^* = \gamma(1 - \beta \cos\alpha) E_\nu \quad (4.27)$$

Since the procedure for  $\bar{\nu}_e$  is the same as for  $\nu_\mu$ , we may rewrite equations (4.21) and (4.22) with new variables  $(\cos \alpha, E_\nu)$ . The Jacobian of the transformation  $(\cos \alpha^*, E_\nu^*) \rightarrow (\cos \alpha, E_\nu)$  is  $\frac{1}{\gamma(1-\beta \cos \alpha)}$ .

$$\frac{d^2\Gamma}{dE_\nu d\cos\alpha} = G_F^2 \frac{M_\mu}{24\pi^3} \gamma(1-\beta \cos \alpha)(E_\nu)^2 [3M_\mu - 4\gamma(1-\beta \cos \alpha)E_\nu] \quad (4.28)$$

$$\frac{d^2\Gamma}{dE_{\bar{\nu}} d\cos\alpha} = G_F^2 \frac{M_\mu}{4\pi^3} \gamma(1-\beta \cos \alpha)(E_{\bar{\nu}})^2 [M_\mu - 2\gamma(1-\beta \cos \alpha)E_{\bar{\nu}}] \quad (4.29)$$

where  $\cos \alpha \in [-1, 1]$  (with no mass  $\nu_\mu$  or  $\bar{\nu}_e$  cannot change the direction of a flight from backwards to forward due to the transformation, no matter how fast  $\mu^-$  flies). For a fixed value of  $\cos \alpha$  it applies  $E_\nu \in [0, \frac{M_\mu}{2\gamma(1-\beta \cos \alpha)}]$  and  $E_{\bar{\nu}} \in [0, \frac{M_\mu}{2\gamma(1-\beta \cos \alpha)}]$ . Above that, we can fix the value of the angle  $\alpha = \alpha_0$  and derive  $\frac{dP}{dE}|_{\alpha=\alpha_0}$  which is the energy distribution of neutrinos emitted at the angle  $\alpha_0$ . The normalization applies:  $\int \frac{dP}{dE}|_{\alpha=\alpha_0} dE = 1$ .

$$\left. \frac{dP}{dE_\nu} \right|_{\alpha=\alpha_0} = \frac{16(1-\beta \cos \alpha_0)^3 \gamma^3}{M_\mu^4} E_\nu^2 [3M_\mu - 4\gamma(1-\beta \cos \alpha_0)E_\nu] \quad (4.30)$$

$$\left. \frac{dP}{dE_{\bar{\nu}}} \right|_{\alpha=\alpha_0} = \frac{96(1-\beta \cos \alpha_0)^3 \gamma^3}{M_\mu^4} E_{\bar{\nu}}^2 [M_\mu - 2\gamma(1-\beta \cos \alpha_0)E_{\bar{\nu}}] \quad (4.31)$$

Expressions (4.28) and (4.29) can be integrated over  $E_\nu, E_{\bar{\nu}}$  respectively in order to obtain  $\frac{d\Gamma}{d\cos\alpha}$ . The flux of  $\nu_\mu$  or  $\bar{\nu}_e$  from a decay per unit of solid angle  $\frac{dP}{d\Omega} \propto \frac{d\Gamma}{d\Omega}$  satisfying  $\int \frac{dP}{d\Omega} d\Omega = 1$  can be easily derived from  $\frac{d\Gamma}{d\cos\alpha}$ :

$$\frac{dP}{d\Omega} = \frac{1}{4\pi\gamma^2(1-\beta \cos \alpha)^2} \quad (4.32)$$

## 4.5 Decay of 3.8 GeV muon

Now we shall apply general results to the decay of  $\mu^-$  with momentum of 3.8 GeV which is considered in the nuSTORM project.

The values of relativistic factors are then:  $\gamma = 36$  and  $\beta = 0.9996$ . Putting them into Eq. (4.30), (4.31), we can calculate and plot the energy distribution of  $\nu_\mu$  and  $\bar{\nu}_e$  for certain values of  $\alpha$ . The case of  $\alpha = 0^\circ$  and  $\alpha = 1^\circ$  are in Fig. 4.5. As we can see, the energy distribution of  $\nu_\mu$  and  $\bar{\nu}_e$  has been only rescaled but otherwise remains the same as in the case of decay of  $\mu^-$  at rest (see Fig. 4.3 for comparison).

The maximal energy of  $\nu_\mu$  and  $\bar{\nu}_e$  emitted exactly in the direction of  $\mu^-$  movement ( $\alpha = 0^\circ$ ) is approximately 3.8 GeV. Nevertheless, the value drops rapidly with increasing  $\alpha$  as we can see in Fig. 4.6. The maximal energy does not exceed 1 GeV for  $\alpha \gtrsim 3^\circ$ .

The intensity of  $\nu_\mu$  and  $\bar{\nu}_e$  beams (i.e. the flux of  $\nu_\mu$  or  $\bar{\nu}_e$  from a decay per steradian as the function of  $\alpha$ ) calculated from (4.32) is in Fig. 4.7. As we can see,  $\nu_\mu$  and  $\bar{\nu}_e$  are emitted with the maximal intensity for  $\alpha = 0^\circ$ ; the intensity decreases with increasing  $\alpha$ , reaching half of the maximal intensity for  $\alpha \approx 1^\circ$ . It follows that most of the  $\nu_\mu$  and  $\bar{\nu}_e$  are emitted in a very acute cone around the direction of a  $\mu^-$  flight. In fact, 28% of  $\nu_\mu$  and  $\bar{\nu}_e$  are emitted within the angle  $\alpha = 1^\circ$ , 61% within  $\alpha = 2^\circ$ , 90% within  $\alpha = 5^\circ$  and 97% within  $\alpha = 10^\circ$ .

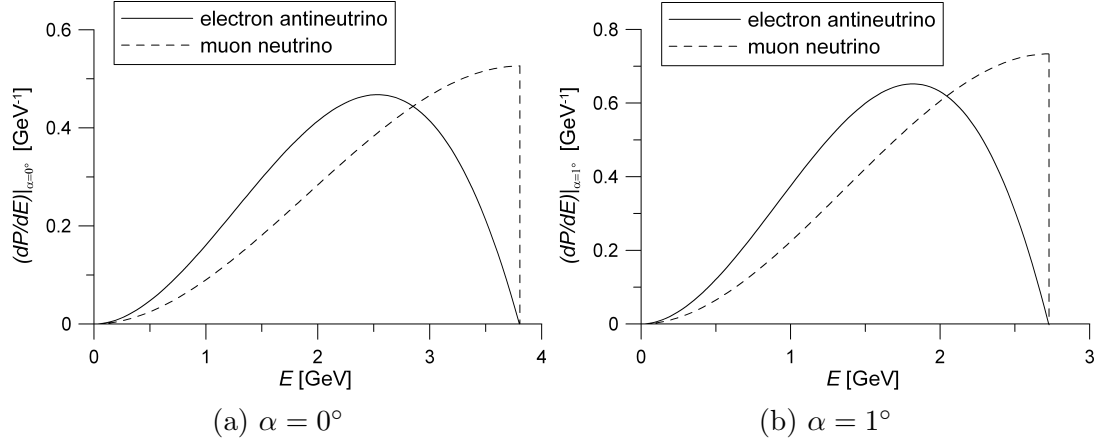


Figure 4.5: Energy distribution  $\left. \frac{dP}{dE} \right|_{\alpha=\alpha_0}$  of  $\nu_\mu$  and  $\bar{\nu}_e$  emitted in the decay of a 3.8 GeV  $\mu^-$  for  $\alpha = 0^\circ$  and  $\alpha = 1^\circ$ . The shape of the distribution is the same as in the Fig. 4.3, only rescaled.

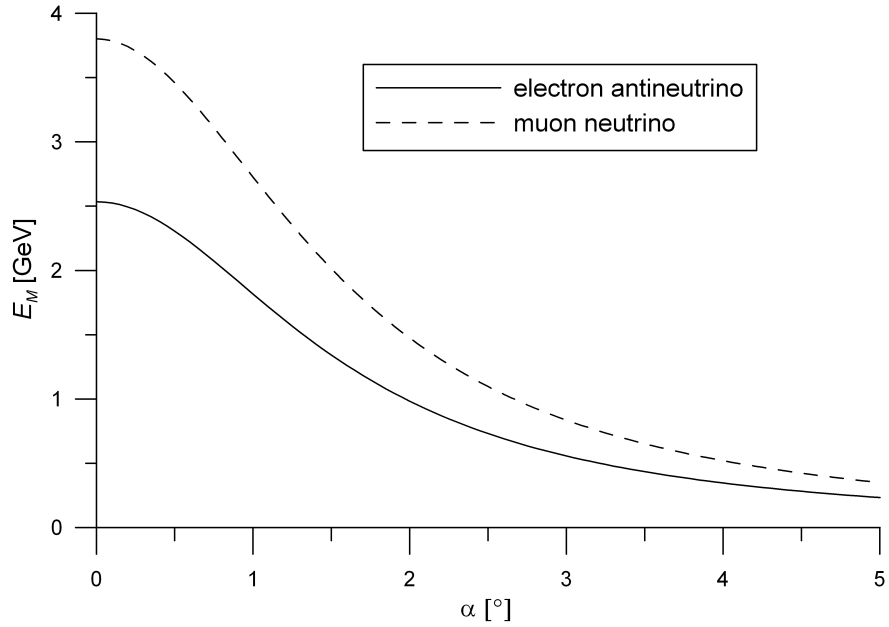


Figure 4.6: The energy  $E_M$  for which the maximal amount of  $\nu_\mu$  and  $\bar{\nu}_e$  is emitted ( $E_M =$  maximal energy and  $2/3$  of maximal energy respectively) as a function of the angle  $\alpha$ .

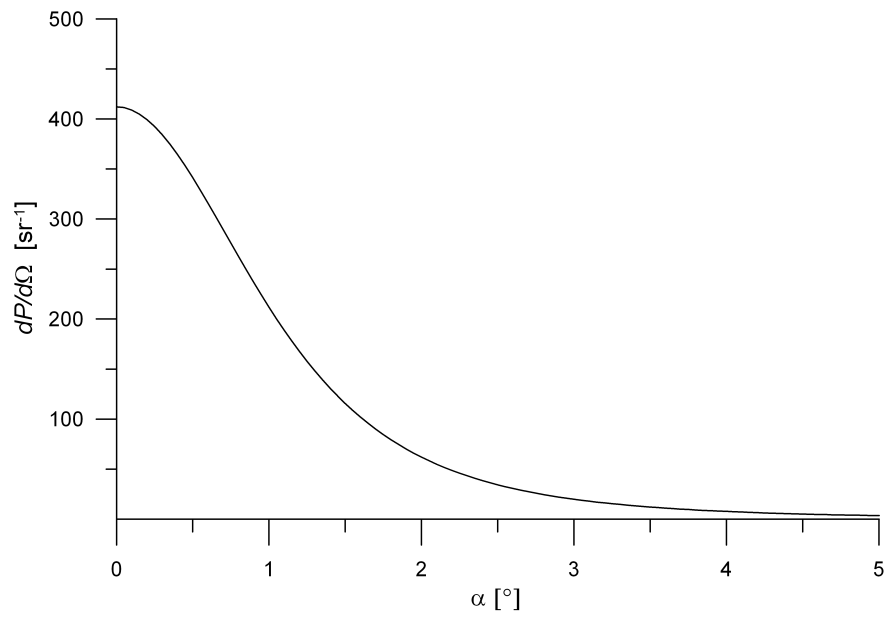


Figure 4.7: The intensity  $\frac{dP}{d\Omega}$  of the  $\nu_\mu$  or  $\bar{\nu}_e$  beam created in the decay of 3.8 GeV  $\mu^-$ .

# Conclusion

In the beginning of this thesis, formalism of neutrino oscillations in the standard three active neutrino framework was presented. That included introduction of the PMNS mixing matrix and derivation of transition probabilities for neutrinos propagating in vacuum. Besides, current values of oscillation parameters were shown with a brief explanation how they were obtained.

In the second part of this thesis, possible CP violation in neutrino oscillations was elaborated in more detail, its effect on oscillation probabilities in general as well as plausible ways of its measurements. Difficulties connected with that (like insufficient knowledge of the neutrino scattering cross section) were discussed along with potential solutions, namely concepts of *beta beams* and the *neutrino factory*. One of the potential implementations of the neutrino factory concept is the nuSTORM facility. Such a facility might, among others, resolve the question of the existence of sterile neutrinos. The possible existence of sterile neutrinos is outlined in the third part of the thesis by providing a brief overview of experiments that can not be sufficiently explained in the three active neutrino framework.

In the last part, I took a close look at a possibility of using muons as a source of neutrinos. I briefly described the concept of the nuSTORM facility and then I focused on the muon decay itself. I calculated the energy distribution of emitted neutrinos in the decay of a muon at rest. It appeared that those distributions are different for  $\nu_\mu$  and  $\bar{\nu}_e$ . While the maximal amount of  $\nu_\mu$  is emitted with energy of  $M_\mu/2$ , for  $\bar{\nu}_e$  it is  $M_\mu/3$ . The reason of such a difference is in the matrix element.

Finally, I altered those results for an unpolarized muon in motion and focused on the 3.8 GeV muons considered in the nuSTORM project. For a fixed angle  $\alpha_0$ , the energy spectra have been rescaled but otherwise remained the same as in the case of the muon decay at rest. The maximal energy of neutrinos (that is the rescaling factor) as a function of  $\alpha$  was described. Beside that, the intensity of the beam was investigated, the maximal flux of neutrinos is emitted along the direction of the muon flight, at  $\alpha \approx 1^\circ$  it drops to a half of the maximum.

# Bibliography

- [1] DAVIDEK, Tomáš and Rupert LEITNER. *Elementární částice od prvních objevů po současné experimenty*. Vyd. 1. Praha: Matfyzpress, 2012, v, 193 p. ISBN 978-80-7378-205-4.
- [2] ZUBER, Kai. *Neutrino Physics* [online]. London: IOP Publishing Ltd, 2004, 432 p. ISBN 0-7503-0750-1.
- [3] THOMAS, Jennifer A and Patricia L VAHLE. *Neutrino oscillations: present status and future plans* [online]. Singapore: World Scientific, c2008, 265 p.
- [4] KAYSER, B. *Neutrino Oscillation Phenomenology*. Apr 9, 2008. e-Print arXiv:0804.1121v3 [hep-ph]
- [5] GONZALEZ-GARCIA, M. C. and Y. NIR. *Neutrino Masses and Mixing: Evidence and Implications*. Jan 8, 2003. e-Print arXiv:hep-ph/0202058v3
- [6] BERINGER, J. et al. (Particle Data Group), *Phys. Rev. D* 86, 010001 (2012). and 2013 partial update for the 2014 edition.
- [7] LEITNER, R. *The Experimental Status of  $\nu_{13}$  from the Point of View of the Electron (Anti-) Neutrino Disappearance Experiments*. Feb 11, 2013. e-Print: arXiv:1302.2409 [hep-ex].
- [8] NUNOKAWA, H. et al. *CP Violation and Neutrino Oscillations*. Oct 18, 2007. e-Print arXiv:0710.0554v2 [hep-ph]
- [9] SIELAFF, J. *Observation of tau neutrino charged-current interactions*. May 16, 2001. e-Print arXiv:hep-ex/0105042v1
- [10] BERNABEU, J. et al. *A combined beta-beam and electron capture neutrino experiment*. Feb 27, 2009. e-Print arXiv:0902.4903v1 [hep-ph]
- [11] GEER, S. *Neutrino Beams from Muon Storage Rings: Characteristics and Physics Potential*. Dec 7, 1997. e-Print arXiv:hep-ph/9712290v1
- [12] KYBERD, P. et al. (nuSTORM Collaboration), *nuSTORM: Neutrinos from STORed Muons*. Jun 1, 2012. e-Print arXiv:1206.0294v1 [hep-ex]
- [13] ADEY, D. et al. (nuSTORM Collaboration), *Neutrinos from Stored Muons nuSTORM: Expression of Interest*. May 7, 2013. e-Print arXiv:1305.1419v1 [physics.acc-ph]
- [14] CASPER, D. *The nuance Neutrino Simulation, and the Future*. Aug 3, 2002. e-Print arXiv:hep-ph/0208030v1
- [15] HEWETT, J. L. et al. *Fundamental Physics at the Intensity Frontier*. May 11, 2012. e-Print arXiv:1205.2671v1 [hep-ex]
- [16] LASSERE, T. *Light Sterile Neutrinos in Particle Physics: Experimental Status*. Apr 29, 2014. e-Print arXiv:1404.7352v1 [hep-ex]

- [17] GREINER, Walter, D BROMLEY and Berndt MÜLLER. *Gauge theory of weak interactions*. 2nd rev. ed. Berlin: Springer, 1996, xvi, 395 p. ISBN 3-540-60227-5.

# List of Tables

1.1	Best fit values of neutrino oscillation parameters . . . . .	9
2.1	Threshold energies for the neutrino-nucleon interaction . . . . .	12